American Journal of Engineering Research (AJER)
e-ISSN: 2320-0847 p-ISSN : 2320-0936
Volume-14, Issue-12, pp-17-39
www.ajer.org
Research Paper Open Access

INVESTIGATION OF ENERGY GENERATION POTENTIAL OF A TIDAL STREAM POWRERED OFFSHORE PLATFORM MOUNTED TURBINE SYSTEM

Osifo Idahosa Terry, Fredrick Chukwunonso Agwazie

Department of Oil and Gas Management, Teesside University School of Computing, Engineering and Digital Technologies. United Kingdom

Corresponding Author: Osifo Terry

ABSTRACT : *This study explored the energy potential of tidal streams using an offshore platform mounted tidal turbine for renewable energy generation. The study was hinged on harnessing eco-friendly marine energy potentials in solving the lingering energy crisis in a developing nation like the United Kingdom with vast marine resources. As part of the study objectives and method, a small scale hypothetical vertical axis tidal turbine and ocean tidal current characteristics were examined using computational fluid dynamics. The interrelationship of operational variables and characteristics of the tidal stream which include tide, flow speed, water density, incident angle of fluid flow, blade size, lift force, instantaneous torque and power were evaluated. Results obtained from the investigation showed that there was a correlation between the analytical and simulated evaluations. The length of turbine blade had a direct effect on its mass, torque power intercepted from the fluid (water). Lift and Power generated by the turbine was directly proportional to the fluid density and speed. Peak torques occur around the mid-design points (0.15 m for Y and Z components). Upper and lower tidal stream speeds of 6m/s and 0.3m/s respectively were used in estimating the deliverable theoretical minimum and maximum powers of the hypothetical turbine and were evaluated as 32.8 Watts and 262400 Watts, respectively. The research however proposes that harnessing the energy potential of tidal turbines could be a promising eco-friendly renewable energy generation when commercially explored.*

KEYWORDS: Energy, Tidal, Flow, Lift Force, England, Lift force, Fluid.

Date of Submission: 06-12-2025 Date of acceptance:15-12-2025

I. INTRODUCTION

Tidal energy uses kinetic energy of ocean currents to generate sustainable electric energy. It has become a promising alternative energy generation globally. Driven by gravitational forces and tidal movements initiated by the moon, [1, 2] it is highly possible to predict its generation. The social-technological, and economic advancement of countries like the United Kingdom (UK) has been greatly aided by this as well as other energy sources including wind, solar, and fossil fuel-generated energy. The advantage of tidal energy is however emphasized based on its predictability unlike other energy generation forms such as wind and solar. Beside growing global energy needs, there is a push for more affordable and clean energy sources that are devoid of harmful pollutants like carbon dioxide, carbon monoxide, and other heavy gases [3]. Countries around the world have jointly made a pact to reduce or eliminate environmental pollution, this has made it necessary to investigate renewable energy sources through the methodical design of energy systems [4]. Water bodies such as rivers, streams, seas, and oceans have been explored over time and have been identified as potential sources of renewable energy sourced from tidal waves and streams. The United Kingdom as a case study has a long stretch of coastline with strong tidal flow or currents which is significant in harnessing marine power. Owing to the developed oil and gas sector of the UK, many of its oil platforms are located offshore. However, it was common thing

for these oil related facilities to rely on fossil energy generation as major power source. This is inimical to the present-day call for the cut in fossil fuel energy use to forestall CO and CO_2 emissions which have largely been attributed to the ozone layer depletion which consequentially causes global warming [3]. To cut emissions, the International Maritime Organization (IMO) unveiled its Initial GHG Strategy. By 2050, the policy seeks to reduce absolute GHG emissions by at least 50% from 2008 levels, with the goal of eliminating them. The UK in pursuit of GHG emissions reduction aims partly to become a leader in emerging tidal energy utilization in its oil and gas offshore facilities. This is particularly so due to the favorable systematic design of tidal energy structures such as tidal stream propelled turbine that can be embedded on these platforms.

Aiming to expand its tidal energy generation capacity with a projection of 120MW from the energy source by 2029, the UK still faces some challenges for the early stages of development of tidal energy generation. Some of these key challenges include high investment cost, harsh marine environment and decisive government support [5]. It is hoped that ocean energy will form another energy supply option for countries and industries seeking to reduce their Green House Gas (GHG) emissions to meet internationally agreed standards and the shipping industry that commands the ocean. This study was aimed at analytically investigating the electricity generation potential of a tidal energy facility mounted on an offshore platform using the UK marine environment as an experimental location. Walker and Thies [6] asserted that the UK has around 50% of Europe's tidal energy resource and with over one hundred wave and tidal current system prototypes under development. Wang et al., [7] conducted research on turbulence induced loads fluctuation of the horizontal axis tidal turbine blade to give insight into the generation mechanism and distribution of excitations on the horizontal axis tidal energy turbine in an unsteady stream-wise flow condition. A small-scale tidal turbine prototype was also used in a field investigation by Zhang et al., [8] off the coast of Scotland to track the structural performance and electrical output of the turbine under actual operating conditions. Phu and Nguyen, [9] conducted investigation and developed a tidal generator prototypes. Perez et al [10] investigated of a tidal turbine performance under various turbulence conditions. The numerical models allowed for the investigating of device performance and loading prior to device deployment and support turbine design optimization at low computational expenses. Adnan et al., [11], developed a laboratory-scale prototype to evaluate the effects of tidal speeds and directions on power output, confirming that even small-scale turbines can yield significant energy under ideal configurations. (March et al., [12] conducted research on Multi-criteria evaluation of potential Australian tidal energy sites. The authors asserted in the research that tidal energy conversion technology is still a modern technology at the research and development stage undergoing field testing before it can reach a successful commercial stage.

II. METHODOLOGY

Parametric analysis of a vertically oriented tidal turbine system was adopted in the study and the materials used include the followings:

i. Hypothetical descriptive model comprising of water bath, ammeter, voltmeter, frequency meter, hose, electric dc pump
ii. Parametric data of existing offshore sites.
iii. Computer aided design and Computational Fluid Dynamics (CFD) analytical software.

The vertical tidal turbine was simulated by computational analysis using CFD and mat lab software. This was necessary to determine the effects and interrelationship of variables on the tidal vertical turbine operation.

III. ANALYTICAL COMPUTATION

Considering design input variables recommended by (Graham et al., [13] the range and mean high waters are expressed as:

i. Range of tide (R) = $H_{wo} - L_{wo}$ (1)

Where, H_{wo} and L_{wo} are high and low water observations.

ii. Mean High Water

The mean high water (MHW) defines the mean high and low water levels averages.
Using the range ratio method [13] MHW can be computed using three simultaneous equations as follows.

$MR_s = R_s \left(\frac{MR_c}{R_c}\right)$ (2)

$MTL_s = MTL_c + (TLs - TLc)$ (3)

$MHWs = MTLs + - \left(\frac{MR_s}{2}\right)$ (4)

where:
R= Range of tide, c = Subscript used to denote control tide station, s = Subscript used to denote subordinate tide station, MR = Mean range of tide; the difference in height between MHW and MLW taken from the NOS data. tenable from DEP/BSM.
TL = Half tide level; the point halfway between HW observed on staff, and LW observed, on staff. Also, TL can be checked by simply adding LW observed on staff, and HW observed on staff and dividing by 2 for each tide station.
MTL = Mean tide level; a tidal datum midway between MHW on staff and MLW on staff. Tenable from NOS Tide Station reference data sheet.
MHWs = MHW on staff; a computed tidal datum at the subordinate tide station. Also, the Mean Low Water (MLW) at the subordinate station can be determined by subtracting MRs from MHWs.

iii. Tidal stream dynamics

For a fluid in free stream the available kinetic energy (E_k) (Bansal, 2017) for any given cross section is expressed as.

$E_k = \frac{1}{2}mu^2$ (5)

Where, m = mass (kg), u = velocity (m/s)
It is the kinetic energy of the fluid that is converted into kinetic energy of the rotor i.e. movement which makes the rotor turn along its axis.

iv. Total Power of the tide $P = \frac{1}{2}\rho Au^3$ (6)

Where, ρ = density of ocean water, A = cross sectional area of the tidal stream

v. Drag force of tide stream (Mason-Jones et al., [14] is expressed as

$D = \int Rx = \int p\cos(\theta)dA + \int \tau_w \sin(\theta)dA$ (7)

Where, R = resulting force of pressure and shear forces, τ = shear force, θ = angle to the upstream velocity.

For the shear stress and pressure distribution, the dimensionless drag and lift coefficients C_D are used and expressed as follows.

$C_D = \frac{D}{0.5Au^2}$ (8)

Drag coefficients for different shapes are presented together with the characteristic area. (Checked from reference data sheet). From equation 3.8, drag force *D* can be computed.

For the tidal energy turbine, the periphery velocity (v) will be lower than the upstream velocity (u). Therefore, equation 3.8 can be modified as follows.

$D = \frac{1}{2}C_p\rho Aw^2 = \frac{1}{2}C_p\rho a(u-v)^2$ (9)

Where; u and v are upstream and periphery velocities respectively, ρ = density

vi. Lift force (L)

The pressure difference between the upper and lower sides of the tide creates a hydrodynamic force (R) acting on the turbine foil. It hits the foil at an angle called the angle of attack (α). It is expressed as; $L = C_L \times q_S$ (10)

where, L = lift force, S= area of the wing, q = dynamic pressure and it is expressed as.

$$q = \frac{rU^2}{2} \quad (11)$$

where, r = fluid density, U = fluid speed

For the velocity continuity through the turbine blade assuming it to be a thin disc, initial velocities equal final velocities, I.e $u_1 = u_2 = u_R$

vii. Momentum of the tidal stream

The tidal stream's total momentum is thought to be constant, which means that the force the rotor applies to the fluid is equal to and opposite to the force the fluid applies to the rotor. This force is referred to as thrustt Alipour et al., [15] as.

$$T = -m(u_\infty - u_w) \quad (12)$$

where $\dot{m}$ is the mass flow rate of the fluid through the rotor and is defined as.

$$m = \rho A u_R$$

Since no work is performed on either side of the rotor the relationship between the pressures and velocities can be expressed for the upstream and downstream side of the rotor respectively by applying the Bernoulli principle as follows.

$$P_o = \frac{1}{2}\rho u_\infty^2 = p_u + \frac{1}{2}\rho u_R^2 \quad (13)$$

$$P_d = \frac{1}{2}\rho u_R^2 = p_o + \frac{1}{2}\rho u_w^2 \quad (14)$$

Therefore, the thrust acting on the rotor in terms of total pressure difference over the rotor is given as $T = A(p_u - p_d)$ (15)

Combining equations (3.13) and equation (3.15) the thrust can now be expressed by:

$$T = \frac{1}{2}\rho A(u_\infty^2 - u_w^2) \quad (16)$$

Considering the mass flow rate from equation (14) and the thrust expressions, the velocities of the model can be expressed as.

$$u_R = \frac{u_\infty + u_w}{2} \quad (17)$$

viii. Rotor hydrodynamics

Considering the interaction between the fluid and the turbine geometrics during operation, the tip speed ratio (TSR) which defines how fast the periphery of the turbine is spinning compared to the free stream velocity can be expressed as.

$$TSR = \frac{\omega r}{u_\infty} \quad (18)$$

Also, the solidity of the turbine (σ) is a measure of how much of the total swept area that is occupied by the turbine at any given moment. For expressions given by ,(Du et al., [16] it is expressed as.

$$\sigma = \frac{Nc}{\pi D} \quad (19)$$

The forces acting on the turbine, including the significant fraction acting in the tangential direction (driving the rotation) and the thrust are solutions to evaluating the turbine performance. These forces are dependent on the angle of attack as well as the non-dimensional Reynolds number expressed as; $Re = \frac{\rho w c}{\mu}$. (20)

The expressions for the tangential and normal force coefficients are expressed as.

$$C_t = C_L \sin(\alpha) - C_D \cos(\alpha) \quad (21)$$

$C_n = C_L\cos(\alpha) - C_D\sin(\alpha)$ (22)

These tangential and normal forces can then be calculated using:

$F_t = \frac{1}{2}\rho w^2 H_c C_t$ (23)

$F_n = \frac{1}{2}\rho w^2 H_c C_n$ (24)

The instantaneous thrust which acts on one of the blades in the direction of flow is expressed as.

$T_i = F_t\cos\theta - F_n\sin\theta$ (25)

By equating the momentum lost by the fluid and the momentum gained by the turbine the only unknown (the induction factor) can be calculated.

Since the axis of rotation is perpendicular to the stream wise direction, the blades experience different conditions in every given azimuth location. The instantaneous torque Q_t from each individual blade and for every azimuthal location is given by Gundersen and Herman., [17] as:

$Q_t = F_t \times r$ (26)

where Ft= instantaneous force and r = the distance of the shaft from the blade outermost tip.

ix. Turbine blade specification

Blade shape and dimension are determined by the aerodynamic performance required to efficiently extract energy, and by the strength required to resist forces on the blade. Rotor et al., [18] asserted that for a given tidal stream speed, turbine mass m(kg) is approximately proportional to the cube of its blade-length L_b

i.e $m = L_b^3$ (27)

Wind power P intercepted is proportional to the square of blade-length.

i.e $P = L_b^3$ (28)

The ratio between the blade speed and the fluid speed is called tip-speed ratio.

In the 360-degree revolution of the turbine shaft, the current flow direction is divided into 180° of passive blade power, and 180° of active blade power. On the passive side of the turbine's shaft, the turbine blade opens to allow flow while on the active side of the shaft, it closes to extract the power from the water current. This model turbine is deemed ideal for harvesting low ocean currents by marine vessels and offers opportunities for durable construction. Vessels using this design should be able to operate in extreme maritime environments and coupled with the periodic hoisting and lowering through the offshore hull necessitates calls for a durable design. Also, the passive-to-active turbine is simple in design and easy to maintain. The blades are capable of harvesting energy from the current at speeds as low as 0.3m/s without the need for an external starting torque, unlike most other tidal turbines which require at least 0.5m/s to start. Wang et al., [19]. These advantages informed the choice of the passive-to-active turbine model for this design. The design concept requires the turbine blades to be hinged at the top of a rectangular frame. The blades have a larger surface area than the frame, so they only flip on one side of the frame. The section of the blade arrangement moving against the current is forced to open in a passive mode while the part in the current direction closes in active mode. This produces a resultant force that turns the shaft in a clockwise direction, as shown in Figure 1.

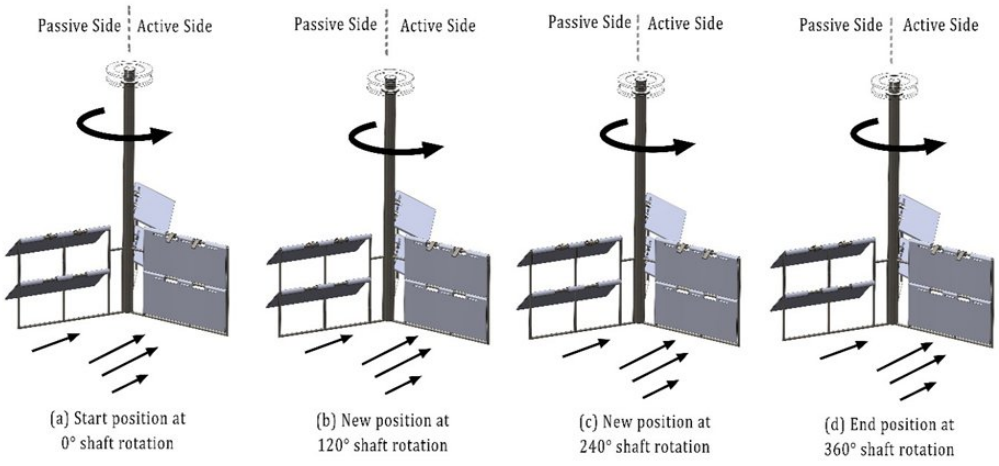

Figure 1. Underwater Tidal Turbine.

The hydrokinetic energy available in any tidal stream is given by

$$P = \frac{1}{2}\alpha\rho AV^3 \qquad (29)$$

Where α = power coefficient

ρ = water density

A = surface area of turbine plate normal to water flow.

V= velocity of water current

According to DURSUN, [20] only 16/27 of this available power can be extracted by a hydrokinetic turbine and this is the maximum power coefficient (α) that a stand-alone tidal current turbine can achieve. Using the Baddas et al., 2017 template a standard sea-going barge measuring 10 meters by 60 meters a blade span of 2 meters could be considered. This length was presumed to be easy to manipulate and wide enough to generate some torque at low current speeds. Mathematically, at 0.3m/s:

$A = 4m^2$, $\rho = 1025kg/m^3$, $V = 6m/s$

Typically, the Gulf stream current, attains speeds of between 0.03m/s at its far depths and 2m/s at the ocean surface. It is the dominant ocean current affecting the UK continental margin. .NASA, [21]. Through ducting technology simulation, the speed of ocean currents could be varied. This principle of ducting was first proposed by Agbakwuru and Ibrahim, [22] for low-velocity flow conditions. Thus, from Equation 1 and substituting values, the lowest theoretical power available to the shaft for the design when blades are fully immersed blades are:

$$P_{min} = \frac{16}{27} \text{ x } \frac{1}{2} \text{ x } 4 \text{ x } 1025 \text{ x } 0.3g^3$$

$P_{min} = 32.8$ Watts

While the highest theoretical power capable of being delivered is

$$P_{max} = \frac{16}{27} \text{ x } \frac{1}{2} \text{ x } 4 \text{ x } 1025 \text{ x } 6^3$$

$P_{max} = 262{,}400$ Watts

$P_{max} = 262.4KW$

This is the maximum theoretical power available on the turbine shaft for conversion into.

IV. Experimental procedure and CFD Simulation.

To validate some significant governing principles of the underwater current power generation turbine, an experimental simulation was carried out along with computer simulations using computational fluid dynamics (CFD) on an experimental model. A 3-bladed (flap) turbine model similar to the Ojarr, [23] model was used for experimentation as shown in Figures 2. A V-shaped water flow guide was directed towards the active blade to initiate a flow velocity. The passive turbine blade was shielded from the incoming water current. The incoming current at the passive turbine is disregarded as being shielded by the model. Also, the force acting against the returning blade on the passive side is disregarded assuming the frame and blades offer negligible resistance to the shaft rotation when the flaps are open. Having fewer blades reduces drag. But a 2-bladed turbine will wobble when they turn to face the current due to variations in its angular momentum. With 3 blades, the angular momentum stays constant because when one blade is incident to the current, the other 2 are at an angle and making the turbine rotate smoothly.

Figure 2 Experimental Vertical Tidal Current Turbine.

Also following the review of the computational equations necessary to define the operation and performance of the underwater power turbine, an analytical and cad simulation of a hypothetical concept is carried out accordingly based on some significant operational quantities which include the following.

i. Lift force.

This is expressed as a function of the angle of attack in which the ocean wave is incident on the turbine blades, the fluid density and the fluid speed. A little consideration will show that from equation (11)

There is a direct relationship between the lift and fluid density and fluid speed. Taking density of water as $997kg/m^3$. The values of the simulation were recorded as shown in Table 1 in the result section. The corresponding graph is also shown in Figure 4.2 of the result section of this work.

ii. Rotor hydrodynamics

The forces acting on the turbine, including the significant fraction acting in the tangential direction (driving the rotation) and the thrust are solutions to evaluating the turbine performance. Normal and tangential forces are acting on the Turbine blades at different conditions in every given azimuth location. These forces are dependent on the angle of attack. The instantaneous torque Qt from each individual blade and for every azimuthal location is dependent on the instantaneous force Ft and the blade length. Active force on the blade across its length can

be verified experimentally according to the governing expression in equation (26). The computations are shown in Table 2 and the corresponding graph in Figure 4.2 in the results section of this work.

iii. Turbine blade specification

Blade shape and dimension are a function of the aerodynamic performance required to efficiently extract energy, and the strength of resisting forces on the blade. Turbine mass m(kg) is approximately proportional to the cube of its blade-length L_b. for given fluid speed. Also, the fluid power P intercepted is proportional to the square of blade-length as depicted in equation (27) and (28) respectively.
The CAS simulated models of the vertical underwater tidal turbine are shown in Figures 3 to 5.

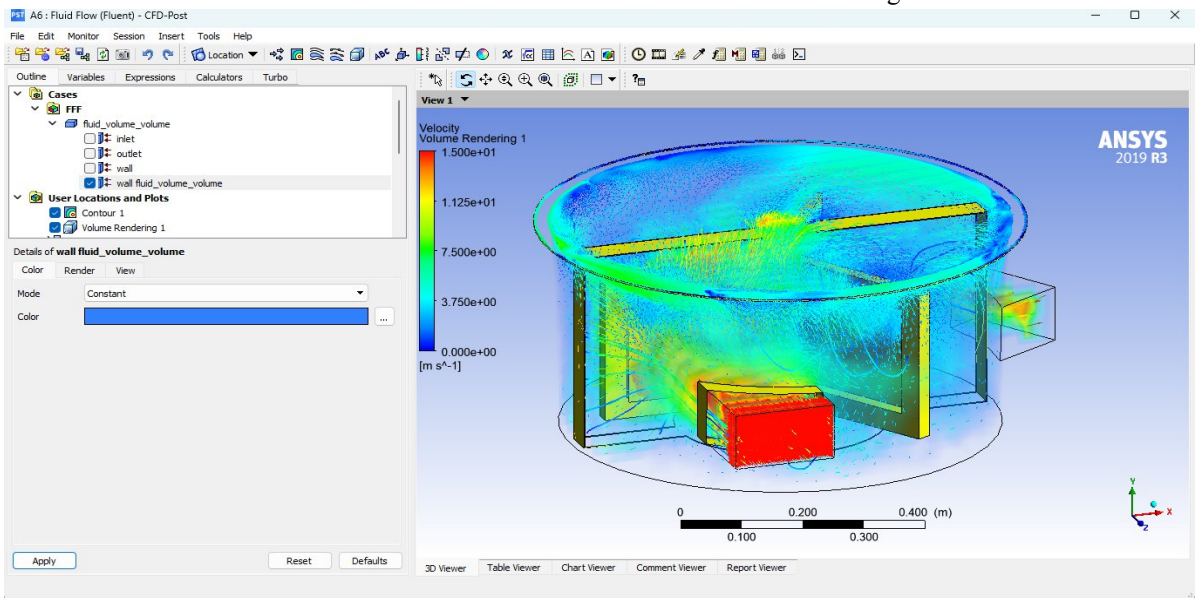

Figure 3 Visualizing CFD Result in ANSYS Environment.

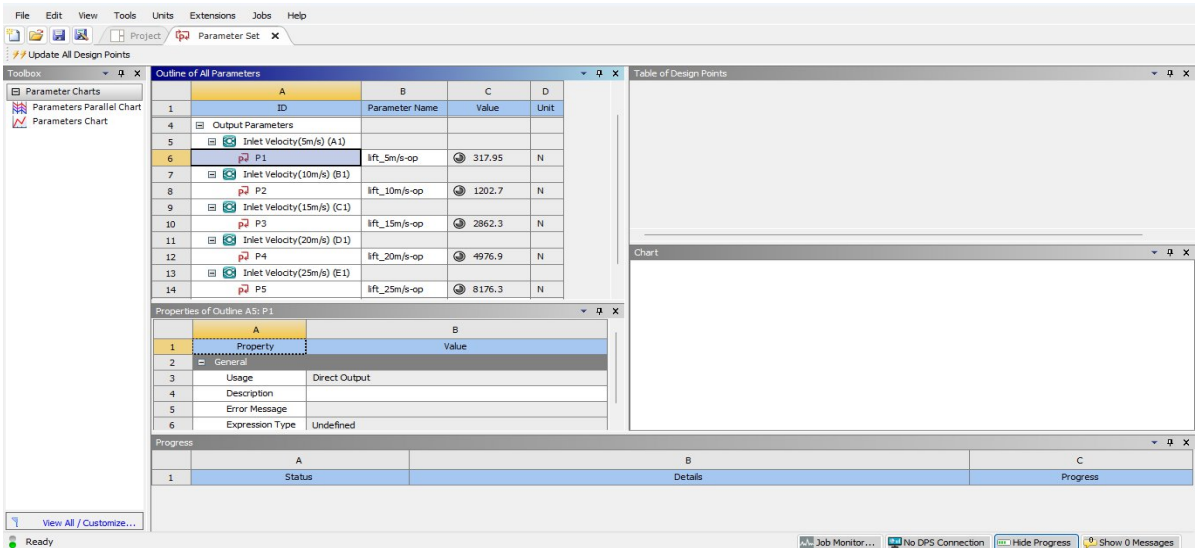

Figure 4 Lift Force Analysis (ANSYS FLUENT)

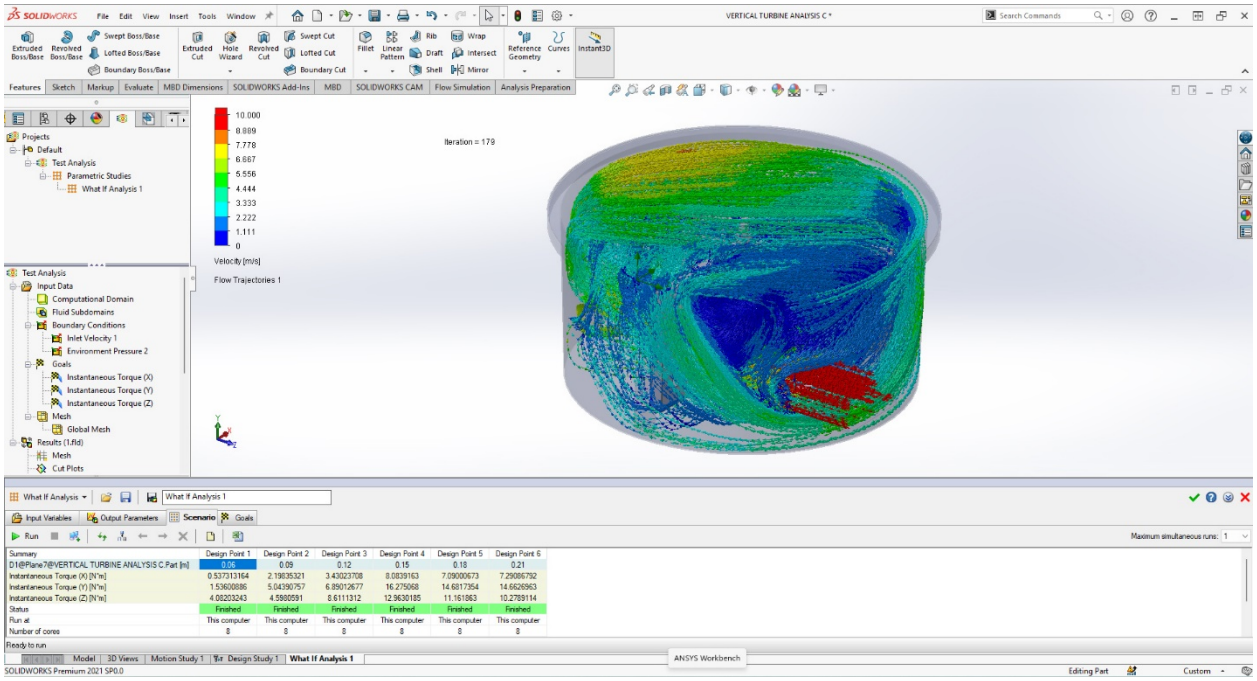

Figure 5 Shaft Torque Analysis. (SOLIDWORKS CFD FLOW SIMULATION)

The motion study settings and results for angular velocity are presented in Figures 6 to 12.

.

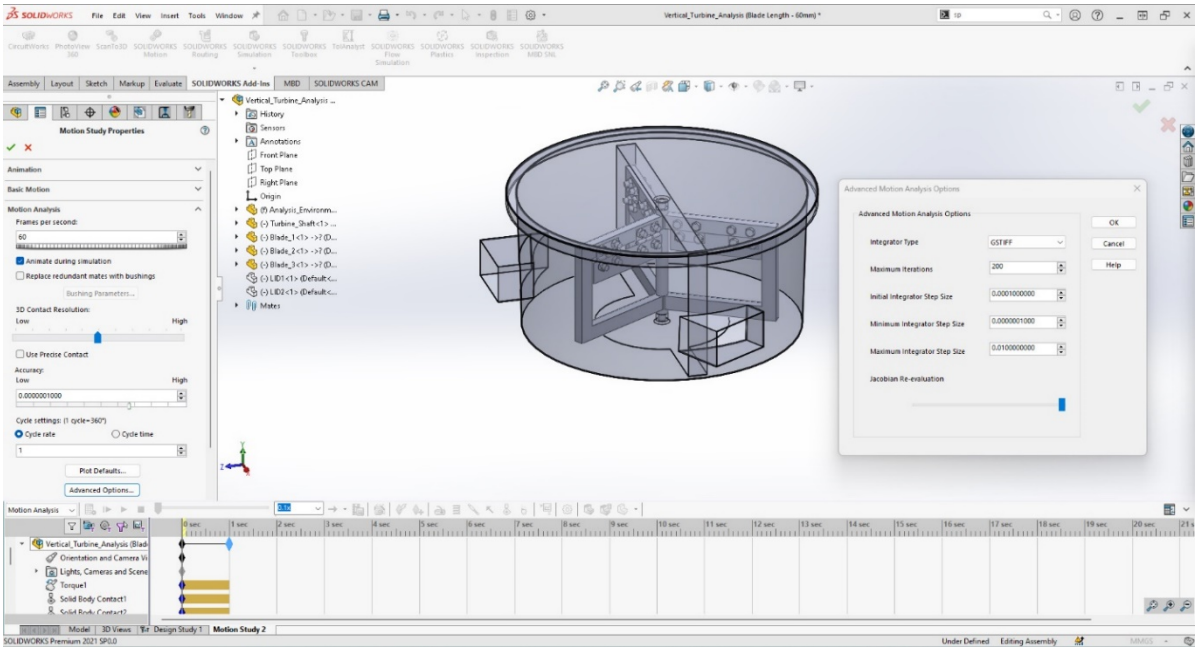

Figure 6 Motion Study Settings and for Angular velocity

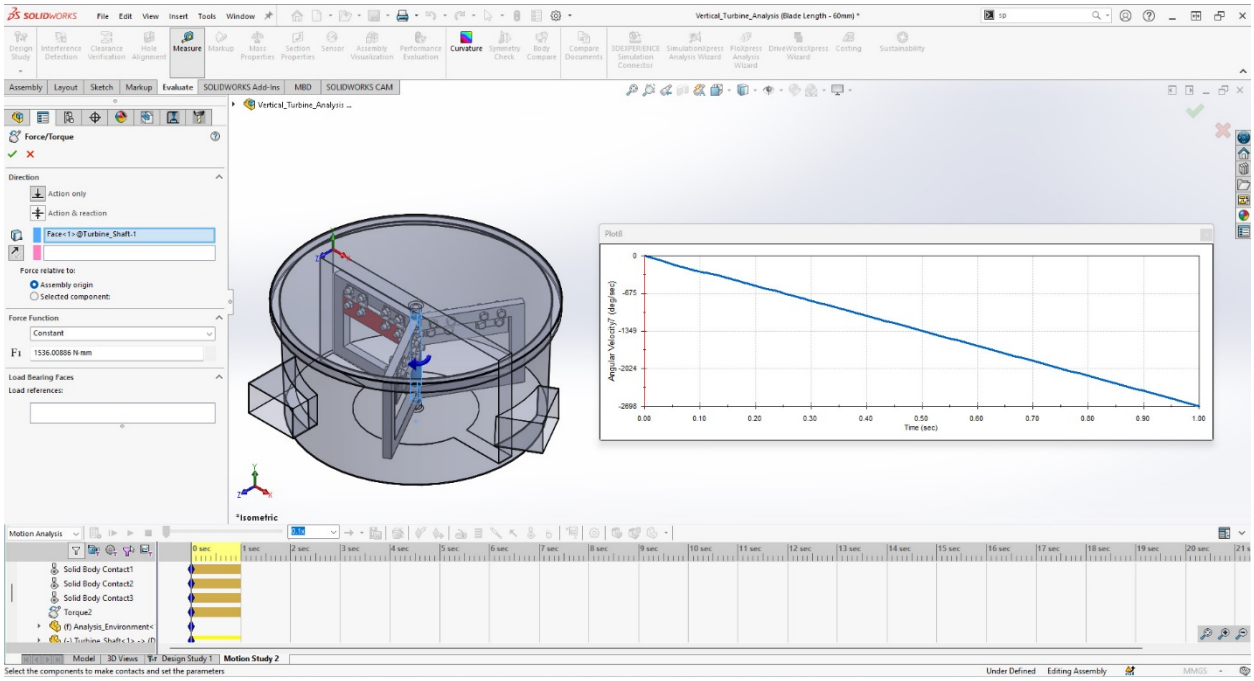

Figure 7 Angular Velocity in Deg/sec for Torque(Y) of 1536.00 Nmm and Blade length of 60mm

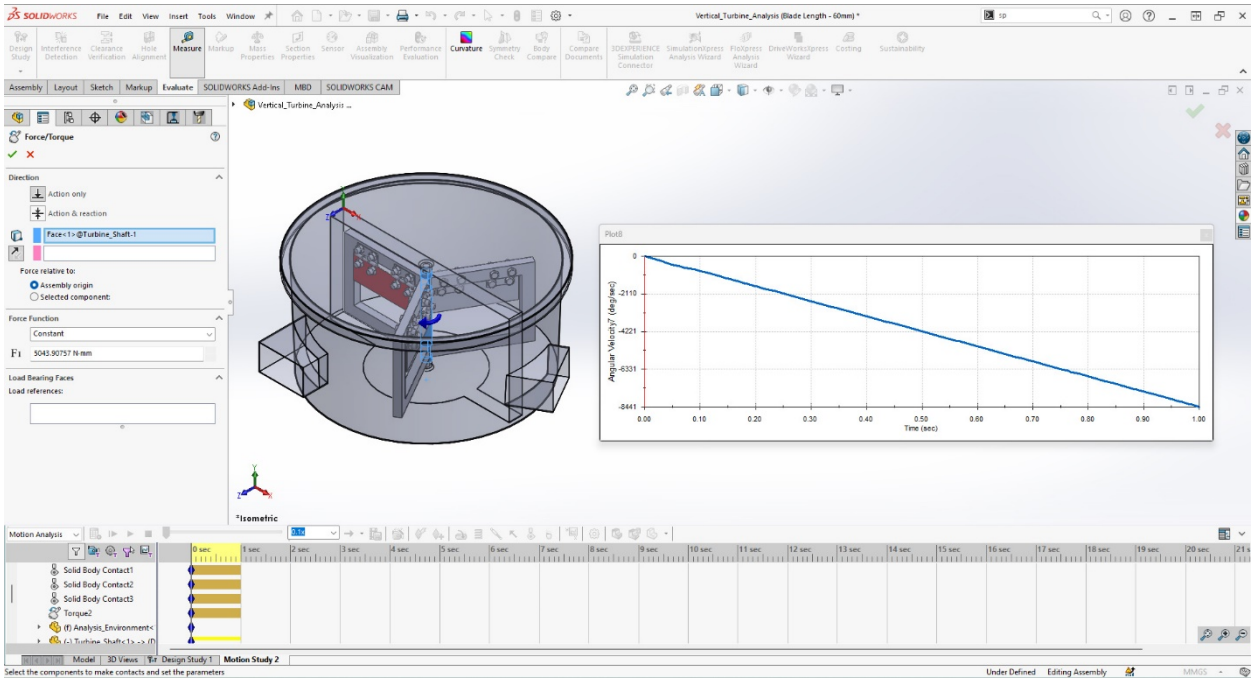

Figure 8 Angular Velocity in Deg/sec for Torque (Y) of 5043.91 Nmm and Blade length of 90mm

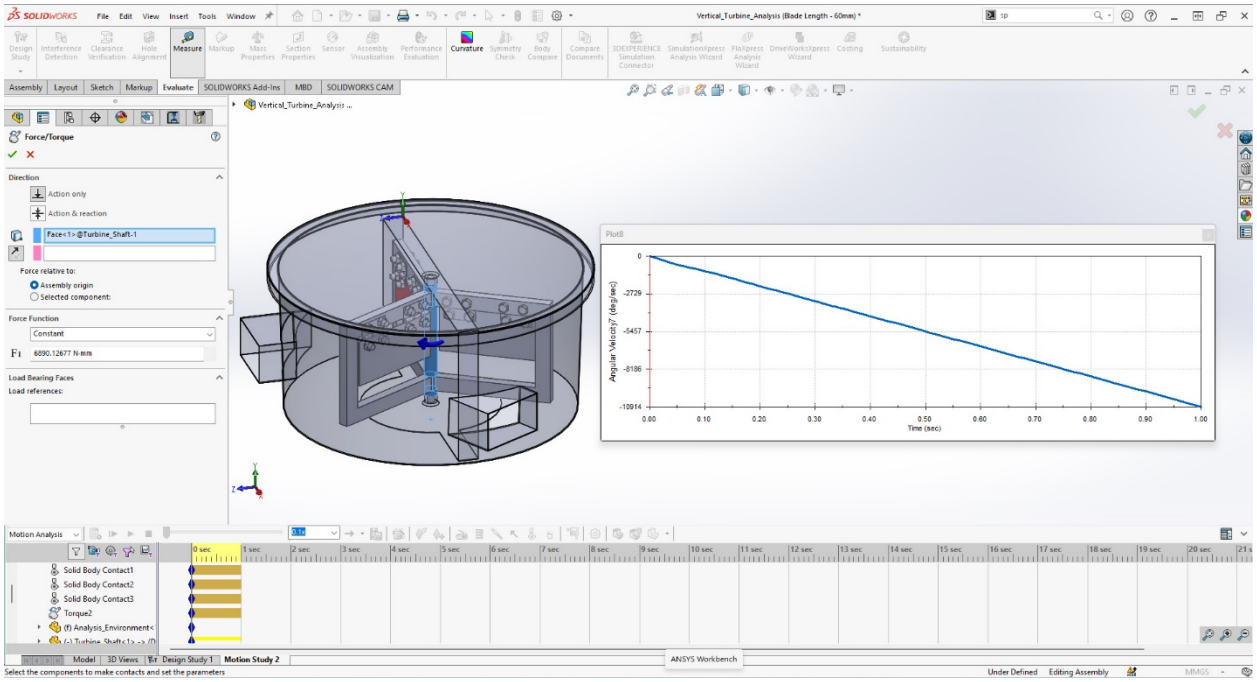

Figure 9 Angular Velocity in Deg/sec for Torque(Y) of 6890.13 Nmm and Blade length of 120mm

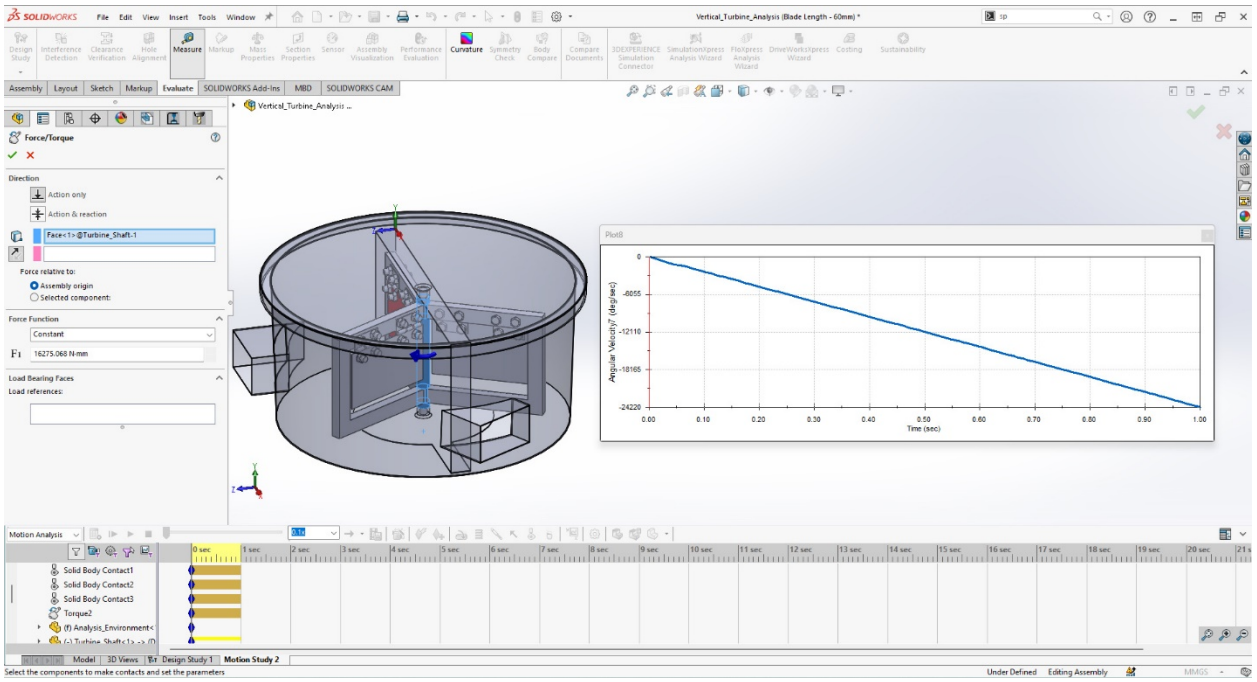

Figure 10 Angular Velocity in Deg/sec for Torque(Y) of 16275.07 Nmm and Blade length of 150mm

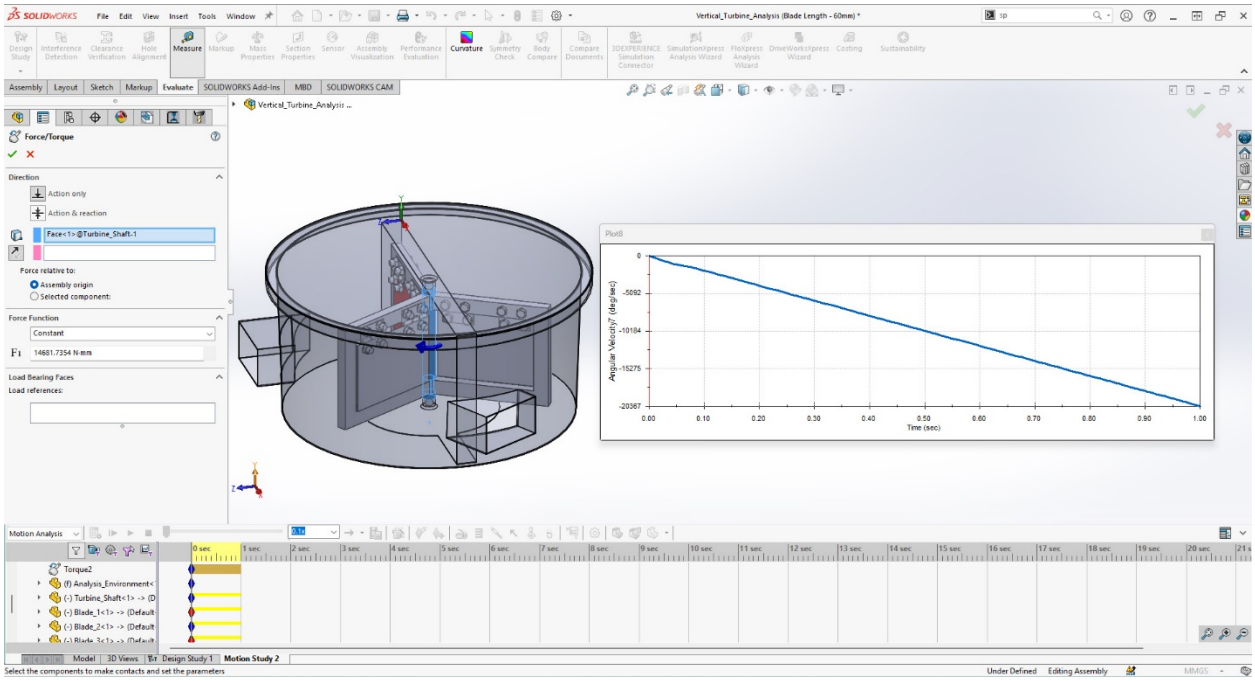

Figure 11 Angular Velocity in Deg/sec for Torque(Y) of 14681.73 Nmm and Blade length of 180mm

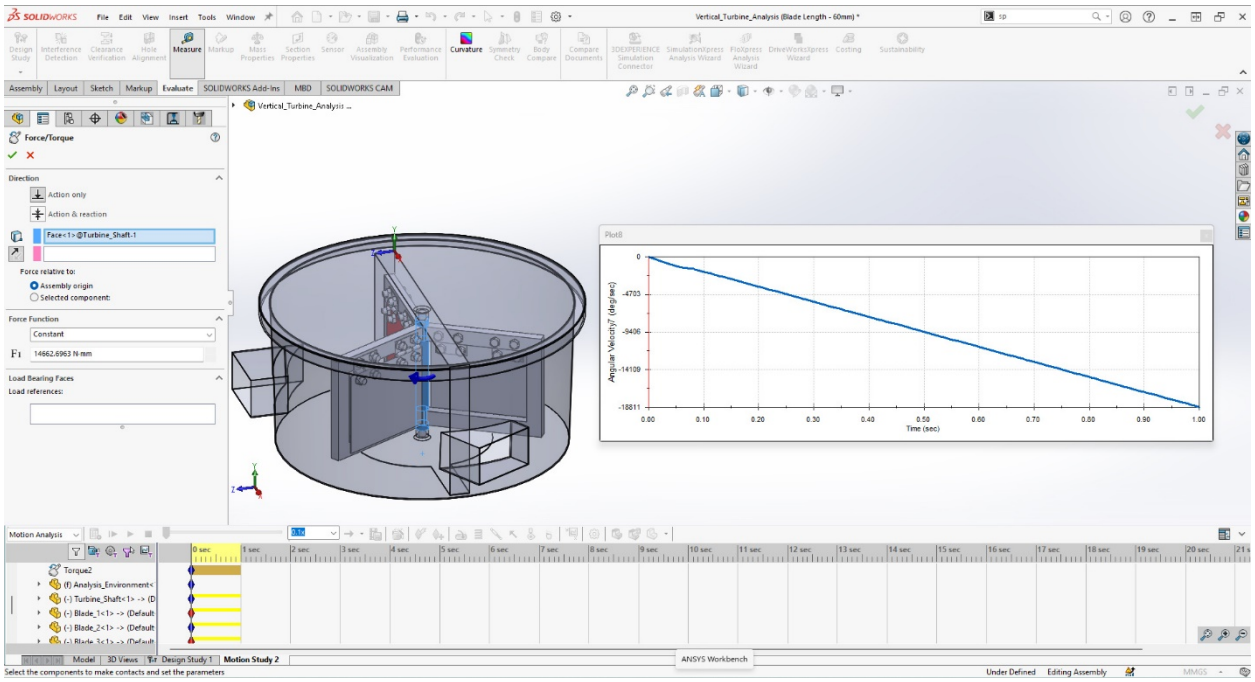

Figure 12 Angular Velocity in Deg/sec for Torque(Y) of 14662.70 Nmm and Blade length of 210mm.

A. The mass properties of the blade of varying length is simulated as shown in Figures 13 to 18.

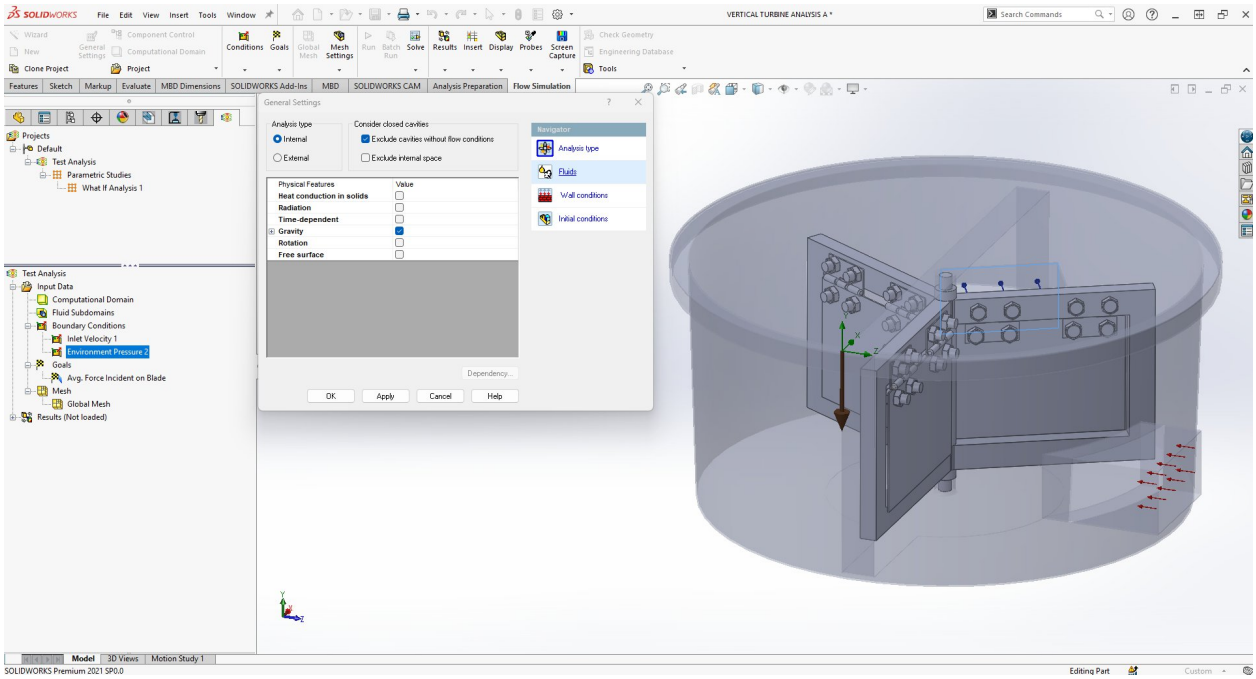

Figure 13 Flow Simulation Setup for Analyzing the turbine Blade Setup

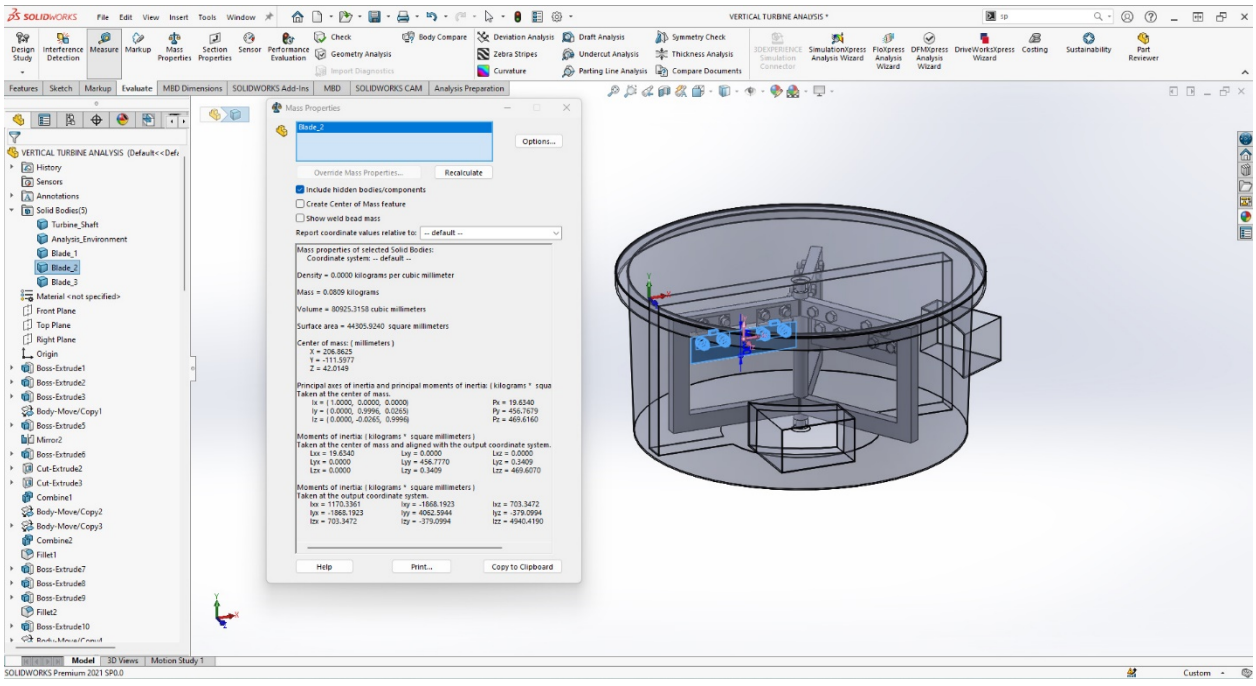

Figure 14 Mass of Blade length 60mm

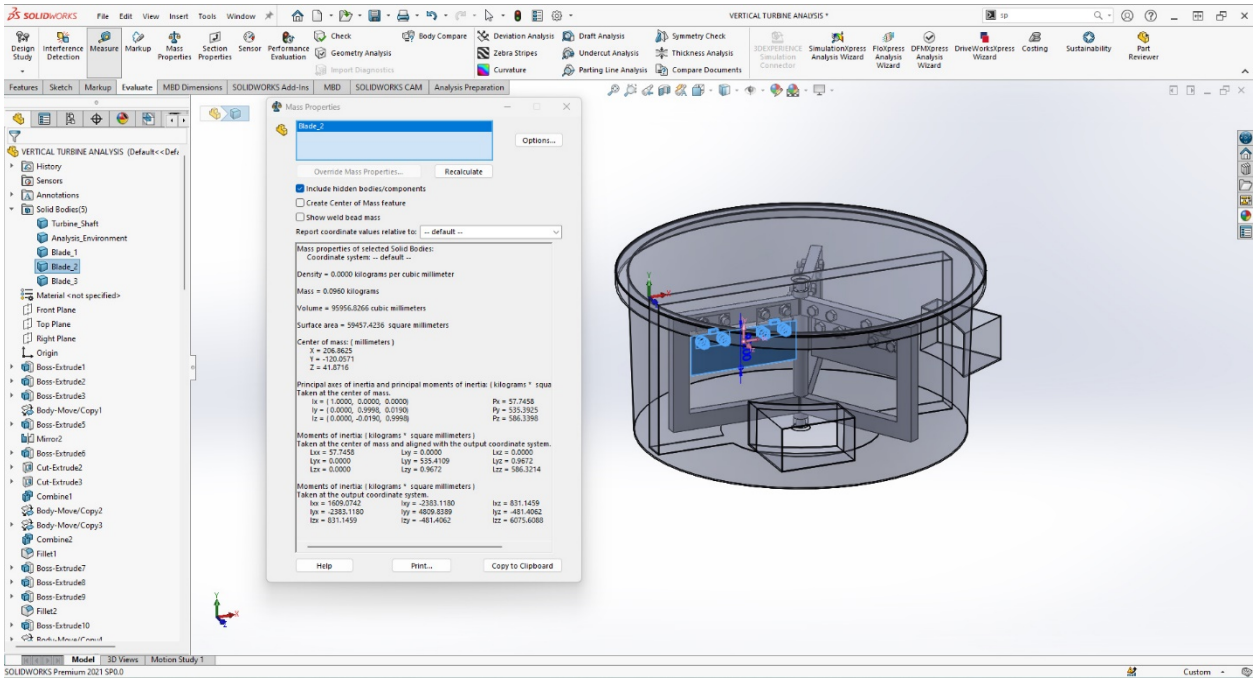

Figure 15 Mass of Blade length 90mm

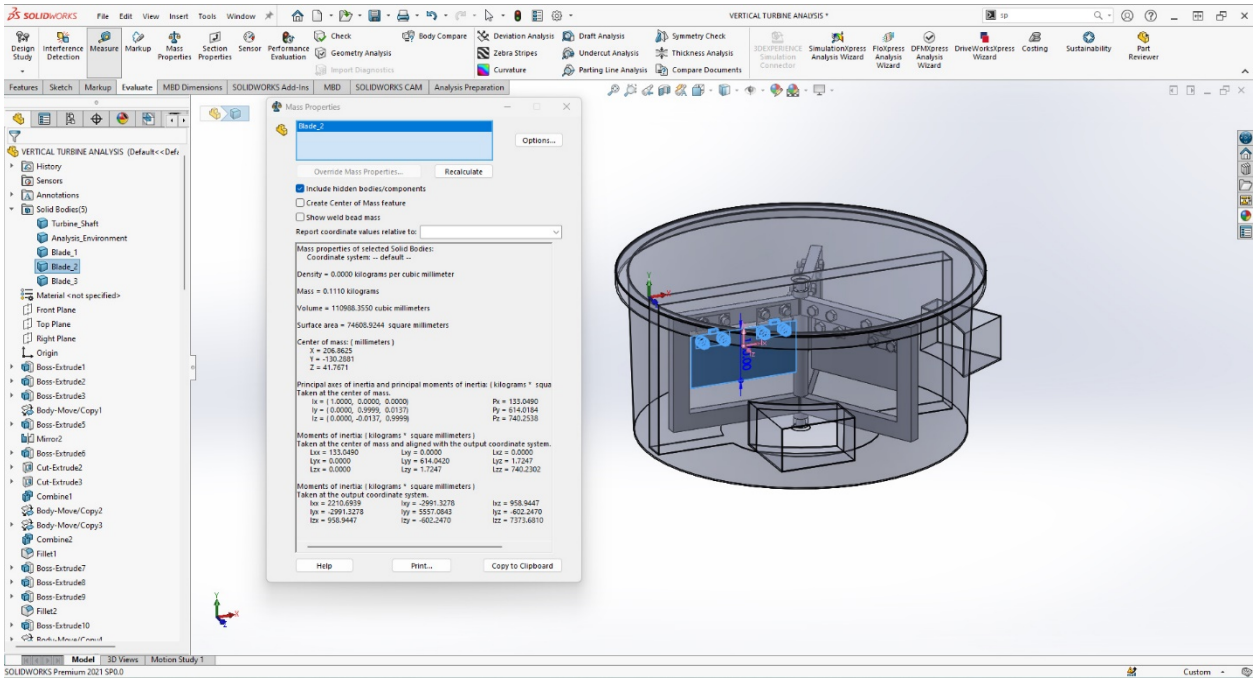

Figure 16 Mass of Blade length 120mm

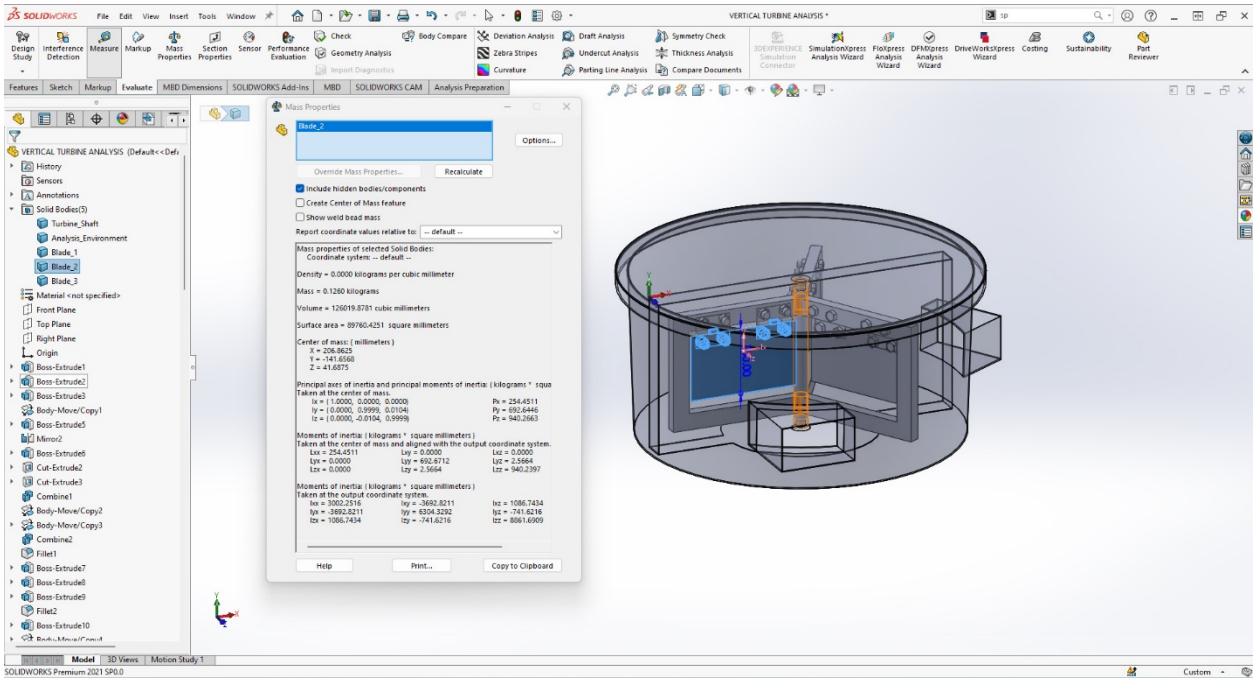

Figure 17 Mass of Blade length 150mm

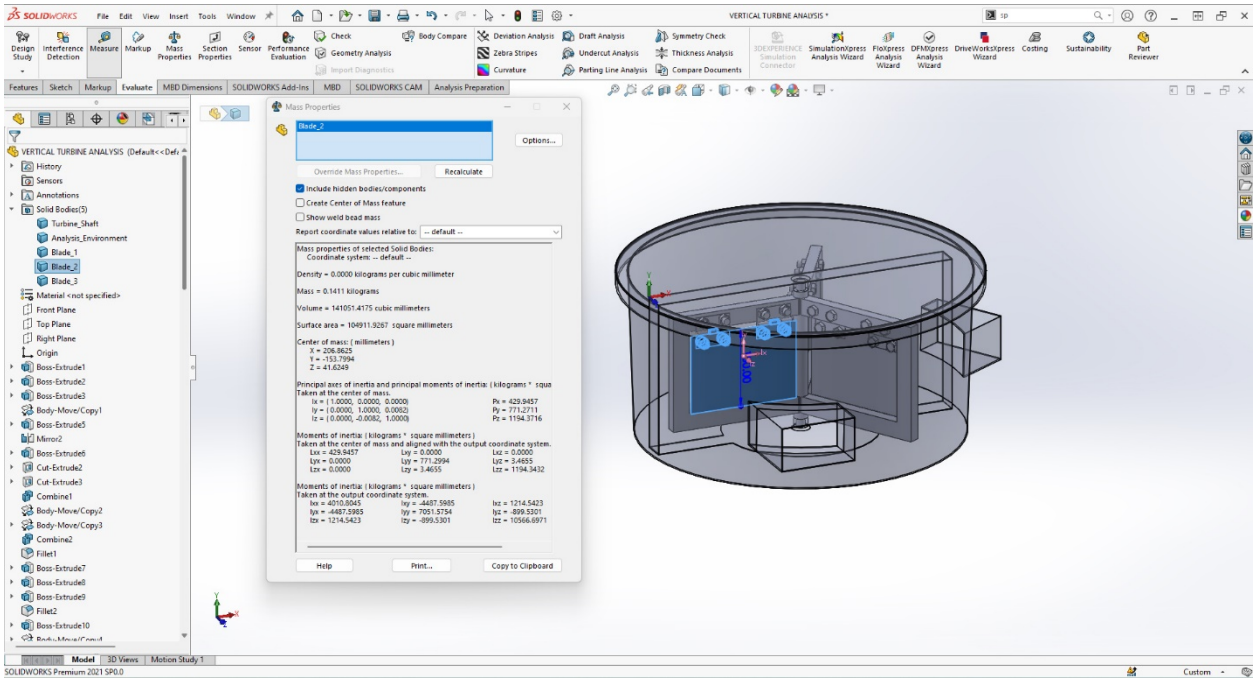

Figure 18 Mass of Blade length 180mm

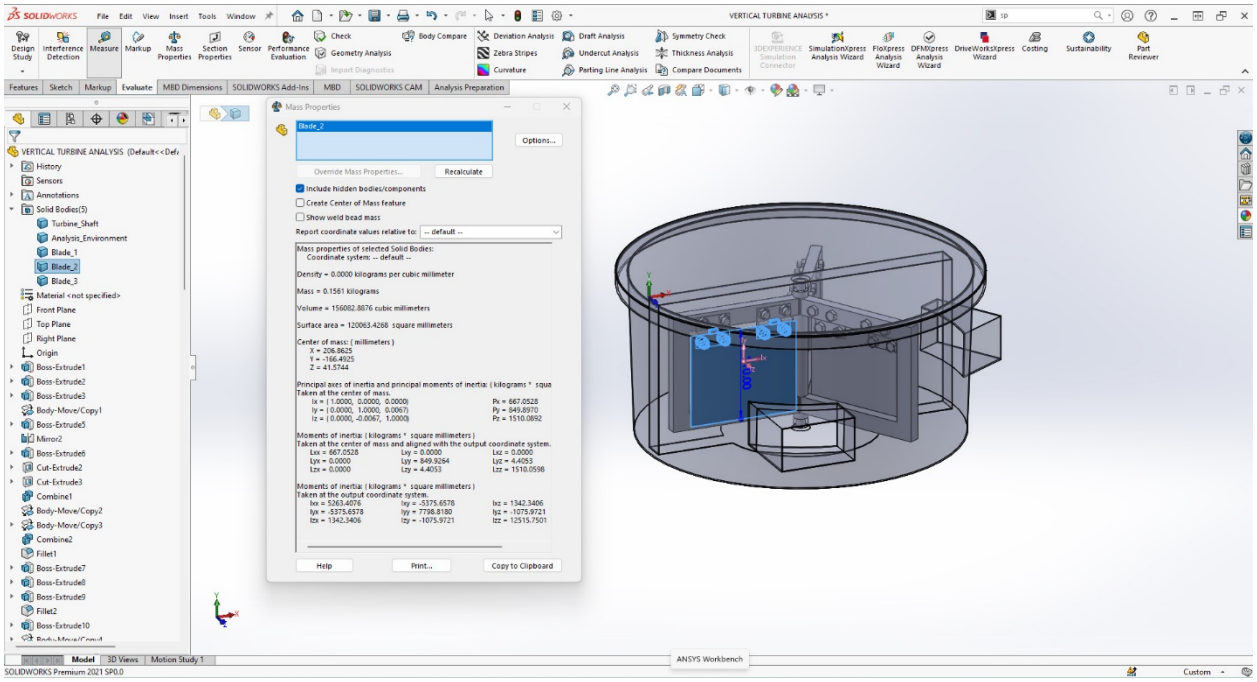

Figure 19 Mass of Blade Length 210mm

.V. RESULT AND DISCUSSION

Effect of fluid density and speed on lift of turbine blade data is shown in Table 1 and graphs are shown in Figures 20 and 21.

Table 1 Value of Lift force

Density of water (kg/m3	speed of water (m/s)	Lift (Analytical)	Lift (CFD simulated)
997	5	2492.5	337.45
997	10	4985	1346.33
997	15	7477.5	3019.98
997	20	9970	5351.76
997	25	12462.5	8347.68

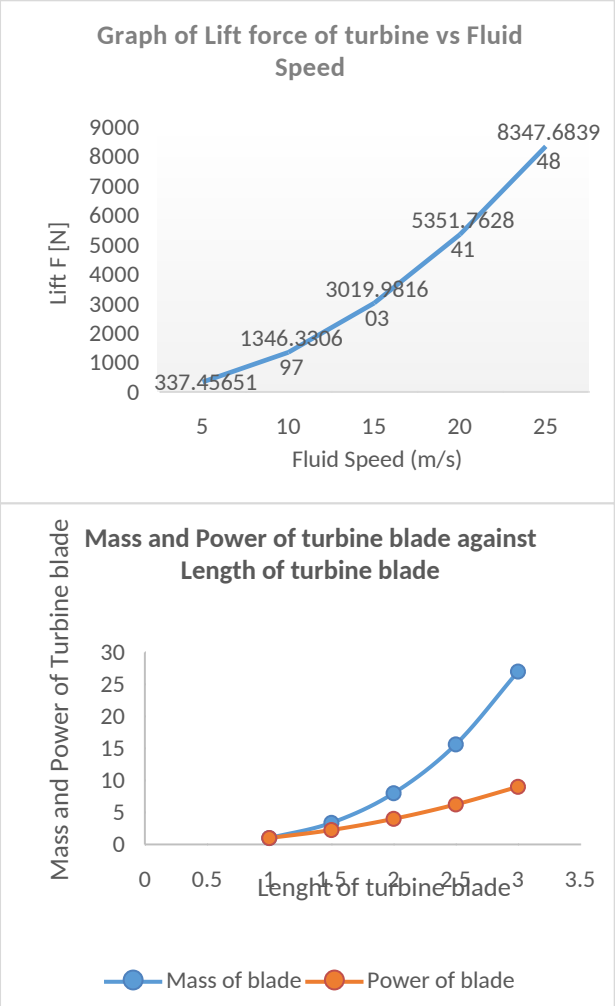

Figure 20. Effect of fluid speed on lift force on underwater current turbine blade (Analytical)

Figure 21 Effect of lift force on under-water Current Turbine blade (CFD)

From Table 1 and Figures 20 and 21, it was inferred that the lift of the turbine which expresses its ability to be pushed through the water current to generate power is directly proportional to the fluid density and speed. During low tides and low water current, there is low energy in the form of torque from the incident water to turn the turbine and this causes inability to generate power. This implies that a forced current generated by a venture can be used to increase speed and direct the water towards the active area of the turbine blade for an effective blade lift. Comparative analysis of the result from the analytical and simulated data shows a correlation in the relationships between the density and flow velocity of water with lift of the tidal turbine blade. However, there was a slight difference between the data as it was observed that the CFD simulated values (Figure 21) were slightly lower and gave a logarithmic relationship rather than a direct linear relationship between the quantities. Table 2

shows the effect of blade length on the instantaneous torque with depicting graphs in Figures 22 and 23.

Table 2 Instantaneous torque against blade length.

		Analytical outcome		CFD Simulated model	
Design Point	Inlet Velocity (m/s)	Blade length (m)	Instantaneous torque Qt (Nm)	Blade length (m)	Instantaneous torque Qt (Nm)
1	10	0.0	0.0	0.06	1.54
2	10	0.2	1	0.09	5.04
3	10	0.4	2	0.12	6.89
4	10	0.6	3	0.15	16.27
5	10	0.8	4	0.18	14.68
6	10	1	5	0.21	14.66

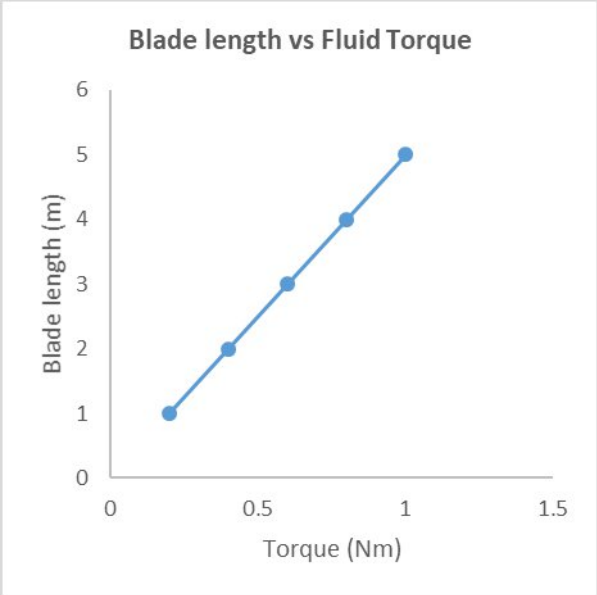

Figure 22 Effect of blade length on Fluid torque. (Analytical).

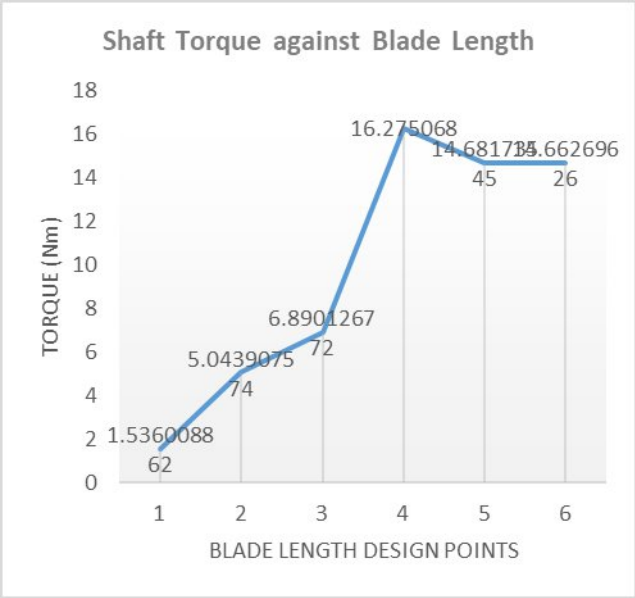

Figure 23. Effect of blade length on Fluid torque (CFD).

From Table 2 and the corresponding graphs in Figures 22 and 23, it can be inferred that the blade length directly affects the torque of the fluid on the blade. The blade area is a derivative of the blade length, hence longer blade length increases the area and active points of incident fluid (water) necessary to initiate torque in the underwater current turbine. The larger the area of contact of the blade surface, the more points of incidence of flowing water current on the active side. Effect of blade length on mass and power intercepted by the turbine blade was computed as presented in Table 4 with corresponding graphs in Figures 24 and 25.

Table 4. Blade Length, Mass and Power relationship.

Analytical Data			CFD Simulated Data		
length of blade (m)	mass of blades(kg)	Power (W) intercepted by blade	length of blade (m)	mass of blades(kg)	Power (W) intercepted by blade P=Torque x Angular Velocity
1	1	1	0.06	0.0809	72.51
1.5	3.375	2.25	0.09	0.0960	742.49
2	8	4	0.12	0.1110	1312.41
2.5	15.625	6.25	0.15	0.1260	6877.65
3	27	9	0.21	0.1561	4813.02

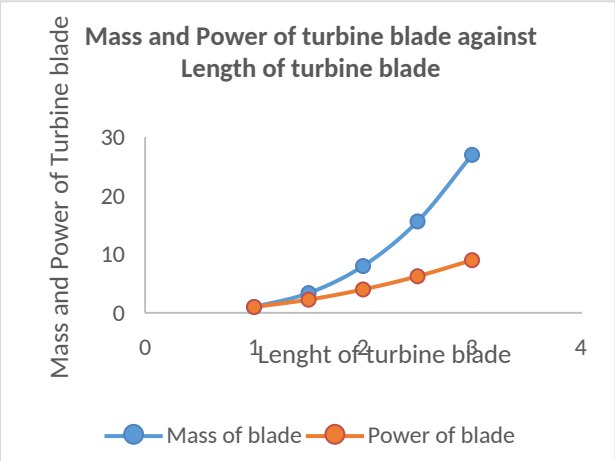

Figure 24. Turbine blade length vs blade mass and power (Analytical).

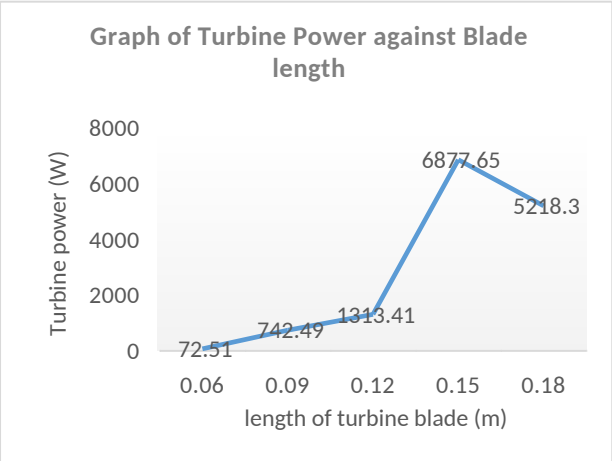

Figure 25. Turbine blade length vs blade mass and power (CFD simulation)

From Table 4 and the corresponding graphs in Figures 24 and 25, it was observed that the length of blade has a direct effect on its mass and power intercepted from the fluid (water). This is also a validation of the increase in torque as blade length increases. The torque has a direct effect on power interception by the blade. From the graph in Figure 24 the blue curve represents the mass of blade while the red curve represents the power intercepted by the blade. They both have a consequential effect on the power generated by the current underwater turbine. As the blade mass, length and fluid torque increases, power generated also increases. The relationship between these quantities was like the CFD simulated values shown in the graph in Figure 25.

.VI. CONCLUSION

As part of set objectives of the study, ocean energy forms were examined, marine vessels and components capable of tapping energy from tidal streams in ocean bodies were identified and finally an experimental tidal stream turbine model was developed, analyzed mathematically and simulated using computer software to ascertain its performance quantities such as power generated, torque, effect of blade mass and area as well as effect of fluid density and speed on the power generation. Following the outcomes of the experimental testing and simulation of the experimental model, it was concluded that harnessing the power of tidal stream through underwater turbine anchored on marine vessel is a viable power generation concept capable of mitigating power generation problems onboard marine vessels and promoting renewable and clean emery sources in the UK, as it is a fuel less energy source devoid of emission of pollutants.

5.0 Acknowledgement/Funding

This study was self-funded by the authors.

6.0 Conflict of Interest Statement

The authors state that they have no competing financial interest or individual associations that could have looked to influence the work described in this article.

.VII. REFERENCES

[1] Energy Information Agency (EIA) (2014). Annual Energy Outlook with Projections to 2035", National Energy Information Centre, EI-30, Forrestal Building, Washington, DC 20585,

[2] Ahmadian, R., Falconer, R. A., & Bockelmann-Evans, B. (2022). Harnessing Tidal Energy in Coastal Waters: A Feasibility Study. *Renewable Energy*, 172, 1443-1454.

[3] Nayak, P, Pandey, R, Singh, S.k, Tejas, M, Acharya, V.N (2019). and Fabrication of Pico Hydro Turbine. *International Journal of Engineering Research & Technology* (IJERT) ISSN: 2278-0181 Volume 7, Issue 07 Published by, www.ijert.org NCMPC - 2019 Conference Proceedings.

[4] Mbaye, A (2022). Review on Energy Audit: Benefits, Barriers, and Opportunities. American *Journal of Energy and Natural*, Volume 1 Issue 1, Year 2022 https://journals.e-palli.com/home/index.php/ajenr.

[5] British Broadcasting Corporation (BBC) (2024). Tidal Energy. https://www.bbc.co.uk/bitesize/articles/z3hwkty#z3n72v4.

[6] Walker, S and Thies, P.R (2021) A review of component and system reliability in tidal turbine deployments. *Renewable and Sustainable Energy Reviews*. 151(12):111495. DOI: 10.1016/j.rser.2021.111495

[7] Wang, P, Li, Kaifu, Wng, L and Huang, B. (2024). Generation and distribution of turbulence-induced loads fluctuation of the horizontal axis tidal turbine blades. *Journal of Physics of Fluids*. 36, 015151.

[8] Zhang, Jisheng; Wang, Guohui; Lin, Xiangfeng; Zhou, Yudi; Wang, Risheng; Chen, Ha (2023). Experimental investigation of wake and thrust characteristics of a small-scale tidal stream turbine array. *Ocean Engineering*, Volume 283, 115038. ISSN:0029-8018 10.1016 2023.115038.

[9] Phu, M, Nguyen, T (2022). Research, Design and Manufacturing of a Prototype Tidal Generator. *Journal of Physics:* Conference Series 2199 (2022) 012014. doi:10.1088/1742-6596/2199/1/012014. IOP Publishing.

[10] Perez, L, Cossu, R, Penesis, I, Grinham, A. (2022). An investigation of Tidal turbine performance and loads under various turbulence conditions using blade element momentum theory and high frequency field data acquired in tow perspectives tidal energy sites in Australia. *Journal of Renewable Energy.* Vol. 201, Part 1. P928-937.

[11]. Adnan, M; Tahir, M A; Jamal, M A; Aslam, Z; Irfan, T; Umer, M (2022) Design, Analysis, and Fabrication of Water Turbine for Slow-Moving Water. *J. Energy Resour. Technol*. 144(8): 082102 (11 pages). Paper No: JERT-21-1723 https://doi.org/10.1115/1.4052773 ISSN:0195-0738 10.1115/1.4052773

[12] Marsh, P, Penesis, I, Nader, J, Cossu, R (2021). Multi-criteria evaluation of potential Australian tidal energy sites. *Renewable Energy* Volume 175, pp453-469. https://doi.org/10.1016/j.renene.2021.04.093

[13]. Graham, D, Sault, M, Bailey, C J (2003). National Ocean Service Shoreline—Past, Present, and Future. *Journal of Coastal Research*. Vol. 38, pp. 14-32.

[14]. Mason-Jones, A.; O'Doherty, D.M.; Morris, C.E.; O'Doherty, T. (2013). Influence of a velocity profile & support structure on tidal stream turbine performance. Renewable Energy. Volume 52, pp23-3. DOI (10.1016/j.renene.2012.10.022).

[15]. Alipour, R; Alipour, R; Fardian, F; Hossein Tahan, M. (2022). Optimum performance of a horizontal axis tidal current turbine: A numerical parametric study and experimental validation *Energy conversion and management*. Volume 258 Pagination 115533 ISSN 0196-8904 0196-8904.

[16]. Du, L, Ingram, G and Dominy, R G (2019). Experimental study of the effects of turbine solidity, blade profile, pitch angle, surface roughness, and aspect ratio on the H-Darrieus wind turbine self-starting and overall performance. *Energy Science & Engineering* 7(6) DOI: 10.1002/ese3.430

[17]. Gundersen, Z. and Herman, D (2014). Turbine design and field development concepts for tidal, ocean, and river application. *Energy Science & Engineering.* Volume 3, Issue 1, p. 27-42. https://doi.org/10.1002/ese3.45.

[18] Rotor, M A, Hefazi, H, and Enano, N (2023). Review on tidal stream energy and blade designs for tropical site conditions and a look at Philippines' future prospects. *Ocean Systems Engineering*. 13(3):247-268. DOI: 10.12989/ose.2023.13.3.247

[19]. Wang, W, Wu, T, Zhao, D, Guo, C, Luo, W and Pang, Y, (2019). Experimental–numerical analysis of added resistance to container ships under presence of wind–wave loads. *PLOS one*14(8):e0221453. DOI: 10.1371/journal.pone.0221453.

[20] Dursun, E. H, (2022). Analysis of performance coefficients in maximum electrical power extraction from stand-alone wind energy conversion system. *Konya Journal of Engineering Sciences.* 10(4):1048-1060 Doi: 10.36306/konjes.1168457.

[21] NASA observatory, (2024). How much does the Gulf of Mexico Contribute to the Gulf Stream? NASA's Scientific Visualization Studio. https://svs.gsfc.nasa.gov/5394

[22]. Agbakwuru, J A and Ukkasha, I U (2019). A novel initiative on vertical-axis underwater turbine suitable for low underwater current velocities. *Underwater Technology*. Vol. 36, No 3, pp 43-51. doi: 1756-0543 10.3723/ut.36.043.